

Direct *ex vivo* measurement of the fluid permeability of loose scar tissue

ANNA FAHLGREN¹, LARS JOHANSSON^{2*}, ULF EDLUND², PER ASPENBERG¹

¹ Department of Clinical and Experimental Medicine, Sweden.

² Department of Management and Engineering, Linköping University, Linköping, Sweden.

Fluid flow is important in many biomechanical models, but there is a lack of experimental data that quantifies soft tissue permeability. We measured the tissue permeability in fibrous soft tissue, using a novel technique to obtain specimens by allowing soft tissue to grow into coralline hydroxyapatite scaffoldings implanted between the abdominal muscle layers of rats.

Key words: permeability, Darcy's law, soft tissue, hydraulic conductivity

1. Introduction

Fluid flow is important in many biomechanical models, e.g., in the models of WEINBAUM et al. [1], where osteocyte excitation is explained in terms of fluid flow, in the models of PRENDERGAST et al. [2], where tissue differentiation is in part decided by fluid flow, and in our own bone osteolysis models [3], [4].

Previous work to determine the permeability of soft tissue has generally considered dense tissue such as cartilage, see, e.g., [5]–[11]. It is more difficult to find published permeability values for less dense types of soft tissue. To our knowledge, the previous measurements with the tissue most similar to the tissue used in the present study are those of LEWIS et al. [12]. However, due to the nature of their experimental setup, their data is not applicable to use in Darcy's law calculations.

In our own efforts to model certain cases of loosening of orthopaedic implants as an event triggered by fluid flow [3], [4], [13], we have been unable to find permeability data for soft tissue types resembling those we wish to model. Therefore, a small study was

initiated where we determined the order of magnitude of the permeability of a tissue type similar to the one in our modelling work. Because of a lack of available data, we believe our results and the technique we have used are of interest, despite the limited accuracy achieved.

In the present paper, a novel technique to produce test specimens was used, to facilitate permeability measurements by direct forcing fluid through the specimens.

2. Methods and materials

2.1. Preparation of specimens

To produce the specimens, porous hydroxyapatite cylinders of the commercially available material Pro Osteon 500, 8 mm long and 8 mm in diameter, were used as scaffolding for soft tissue ingrowth. The cylinders were fitted into stainless steel tubes to allow tight fitting into brass holders used during the perme-

* Corresponding author: Lars Johansson, Linköping University, SE-581 83 Linköping, Sweden. Fax: +46 13 28 11 01, e-mail: lars.johansson@liu.se

Received: June 24th, 2011

Accepted for publication: April 4th, 2012

ability measurements (figure 1). In each of eight rats, the cylinders (in their steel tubes) were implanted between the abdominal muscle layers and left in place to allow tissue ingrowth. After six weeks, the specimens were carefully removed from the muscle and trimmed off soft tissue protruding from the steel tubes. A typical specimen with ingrown tissue removed from its steel tube is shown in figure 2. To minimize the risk of any flow developing at the interface between the steel tubes and the specimens, the specimens and tubes were handled as a unit during the actual experiments. Nevertheless, despite a tight fit between the cylinders and specimens, some near-wall flow cannot be ruled out, leading to an overestimation of permeability.



Fig. 1. The central part of our experimental setup, showing the hydroxyapatite scaffolding, with its stainless steel tube and the brass holder used when applying fluid pressure



Fig. 2. A tissue sample with the steel cylinder removed, showing tissue ingrowth into the scaffolding

After the permeability measurements, the cylinders were processed for demineralised histology, using sections parallel to the axis of the cylinder and haematoxylin/eosine staining. A micrograph of typical tissue in our specimens is shown in figure 3. It is seen that interconnected pores of the scaffolding contain a loose fibrous tissue with spindle-shaped cells and numerous wide vessels.

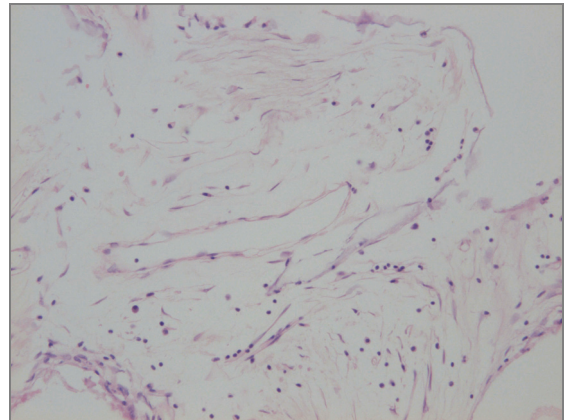


Fig. 3. Light micrograph of tissue from hydroxyapatite scaffolding ingrowth experiments. Note the scant cells (dark nuclei, the rounded ones belong to inflammatory cells) with the loose network of extracellular matrix

Towards the center of the scaffolding, the fibrous tissue becomes scant, with an increasing proportion of round cells and bleeding, so that, on average, the central third could be regarded as having no fibrous tissue ingrowth. The length of tissue ingrowth, Δx in equation (2), was measured under the microscope at this stage.

All experiments were carried out in accordance with institutional guidelines for care and treatment of experimental animals.

2.2. Permeability measurements

The overall experimental setup is outlined in figure 4. A sample holder was designed to allow direct measurement of fluid permeability (figure 1). The sample holder was designed with internal o-ring seals fitting against the rims of the steel tube containing the sample, to provide a leak-proof fluid path.

To provide pressure, the sample holder was connected to a syringe filled with lactated Ringer's solution and rigged into a small tensile test machine set at a constant compressive load. The pressure was monitored directly using a pressure transducer connected to the system at the upstream side of the sample holder. The pressure varied from 139 kPa to 308 kPa, but was very nearly constant during the collection of each tube of fluid. The pressure levels were in part dictated by the practicalities of our experimental setup, but are similar to the pressures in our fluid-induced osteolysis experiments [3], [4].

After a short wait to allow steady-state conditions to develop, fluid was collected at the downstream end of the sample holder. Several Eppendorf tubes were

collected for each tissue sample, measuring the time required to fill each tube by a hand-held stopwatch. The collection time for a tube was between 10 and 167 seconds, with one outlier at 624 seconds.

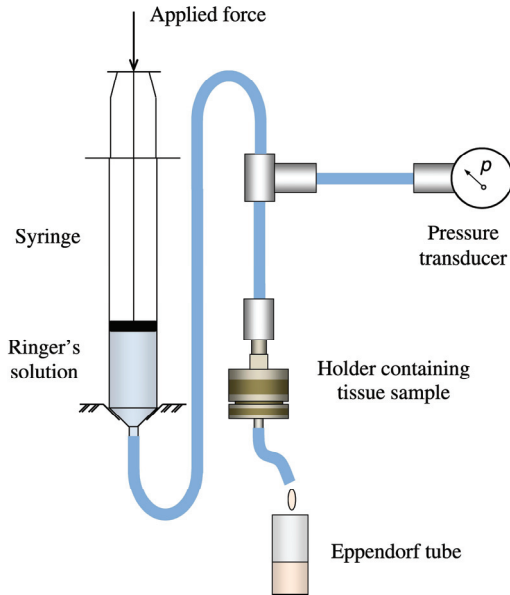


Fig. 4. The overall experimental setup

2.3. Interpretation of data

The measurements were interpreted in terms of a modified form of the one-dimensional Darcy's law:

$$\frac{Q}{fA} = -c \frac{dp}{dx}, \quad (1)$$

where:

Q is the volumetric flow rate,

A is the overall cross-sectional area (including both scaffolding and soft tissue),

dp/dx is the pressure gradient,

c is the permeability to be determined,

f is the porosity, i.e., the fraction of soft tissue volume to total volume (tissue plus scaffolding) of the specimen.

The inclusion of the porosity in equation (1) is a modification of the standard form of Darcy's law to exclude the part of the specimen cross-sectional area taken up by the scaffolding material. It is assumed that no fluid flows through the scaffolding material, so that $Q/(fA)$ is the average velocity based on soft tissue area fA , and c is the permeability of the pure soft tissue as used by JOHANSSON et al. [3]. It is assumed here that the area fraction of soft tissue is equal to the volume fraction (i.e., the porosity). Referring to equation (1), the permeability was calculated from experimental data as

$$c = \frac{\Delta m \Delta x}{\rho \Delta t f A \Delta p}, \quad (2)$$

where:

Δm is the mass of fluid collected in a test tube during the time interval Δt ,

Δp is the pressure drop across the specimen length Δx .

The ingrowth of tissue into the cylinders was not complete, so Δx was measured for each specimen at the histological investigation. The cross-sectional area A was calculated from the nominal 8 mm diameter of the specimens and for ρ , the density of the fluid, the value of 998 kg/m^3 for water was used. Physical data for Pro Osteon 500 has been reported previously, see, e.g., HADDOCK et al. [14]. It was assumed in the present calculations that f had the value of 0.68.

Using equation (2) with SI-units gives permeabilities in units of m^4/Ns . Permeability data is sometimes reported in units of m^2 , using a definition of permeability corresponding to multiplying our values with the viscosity. Using the viscosity for water, permeability values in m^4/Ns will be 1000 times larger than corresponding values in m^2 , c.f. O'BRIEN et al. [15].

3. Results

23 permeability values were obtained, using three tubes for each of the eight specimens, with only two tubes available for one of the specimens. A mean value was calculated for each specimen. The range of these mean values was $c = 0.67-13 \times 10^{-11} (\text{m}^4/\text{Ns})$ with a median of $3.0 \times 10^{-11} (\text{m}^4/\text{Ns})$. It can also be observed that the range of $1.6-5.0 \times 10^{-11} (\text{m}^4/\text{Ns})$ covers half of the data (12 of 23 values).

To investigate a possible change in permeability as fluid is forced through the tissue, the permeability was plotted as a function of the amount of fluid that had passed through the specimen, shown with markers in figure 5. This was possible since each collected tube was clocked individually. The curves seem to indicate that there is an increase in permeability as more fluid is forced through the tissue. This might be simply because the flow affects the tissue physically, perhaps by flushing out minute amounts of tissue or by increasing the fluid content of the tissue. Considering low flow rates in vivo, any such mechanism would reach a steady state, and the limiting case of our measurements would be of interest. To estimate this, the curves were extrapolated to the limit of no fluid having passed the sample, using a linear least squares fit shown as

lines in figure 5. The range of extrapolated permeability values is $c = 0.31\text{--}7.8 \times 10^{-11}$ (m^4/Ns) with a median of 1.6×10^{-11} (m^4/Ns).

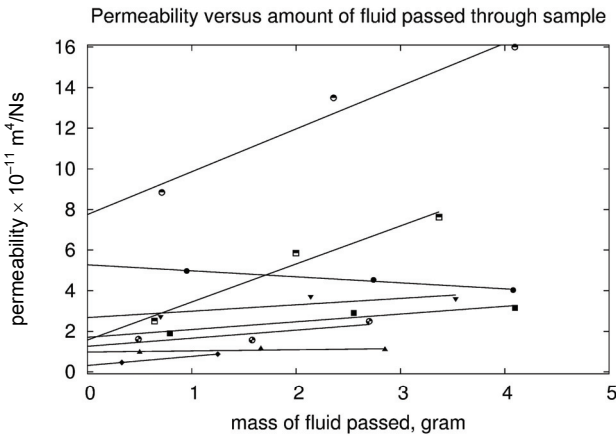


Fig. 5. Evolution of permeability.
Markers represent experimental data,
lines are linear least squares fits

4. Discussion

There is a limited amount of permeability data available for soft tissue, and the available data typically deals with tissue types such as cartilage with very low permeability. The data obtained for such tissue types tend to be within an order of magnitude or so of 10^{-15} (m^4/Ns), see, e.g., [5]–[11].

In the present paper, we studied a much more permeable tissue type that appears in the early stages of ingrowth into an artificial scaffolding. We believe that such tissue can serve as a model for, e.g., granulation tissue in wound healing. Judging by the histological appearance, the content in each single pore of the scaffolding was mainly homogeneous, i.e., its structure was not much dependent on the vicinity of a hydroxylapatite surface. It should be pointed out that the results represent an average of denser fibrous tissue near the cylinder openings and looser tissue deeper inside the scaffolding.

As could be expected, the type of the tissue used in the present paper shows a much higher permeability than cartilage, about 3×10^{-11} (m^4/Ns), i.e., it is some three to five orders of magnitude more permeable than cartilage.

A different class of tissue where a considerable amount of data is available in the literature is tumor tissue. The permeability of such tissue is typically intermediate between cartilage and the tissue studied in the present paper. For example, the permeability

values for human colon adenocarcinoma (LS174T) tissue in [16]–[18] as well as for several other tumor types [16], [19] are within an order of magnitude of 10^{-13} (m^4/Ns). The permeability of murine melanoma tissue (B16.F10) in [20] is even higher than our values, at about 5×10^{-11} (m^4/Ns) (according to our interpretation of figure 3a of that paper). Compared to these reports, it can also be noted that the variation in permeability between different samples in the present work is not exceptionally large.

An important point is the dependence of the permeability on various factors, i.e., the limits of validity of equation (1). Thus, the dependence of permeability on tissue deformation is considered by NETTI et al. [16], while the effect of irradiation is studied by ZNATI et al. [17]. In the present paper, we have studied the change of permeability as more fluid is forced through the sample, concluding that the permeability will increase as more fluid passes through the tissue, see figure 5.

Fluid flow through tissue described as a combination of fibrocartilage and fibrous tissue was studied by LEWIS et al. [12], who examined tissue below artificial knee implants in dogs. Unfortunately, due to the nature of their experimental setup, no direct comparison is possible. We estimate, however, that their data correspond to about one or two orders of magnitude lower permeability than in our experiments. This difference is probably due to the fact that a large portion of the interface in that study consisted of dense fibrocartilage and, to some extent, of bone, whereas we studied the loose fibrous tissue typical of rather early healing.

References

- [1] WEINBAUM S., COWIN S.C., ZENG Y., *A model for the excitation of osteocytes by mechanical loading-induced bone fluid shear stress*, Journal of Biomechanics, 1994, 2, 339–360.
- [2] PRENDERGAST P.J., HUISKES R., SOBALLE K., *Biophysical stimuli on cells during tissue differentiation at implant interfaces*, Journal of Biomechanics, 1997, 30, 539–548.
- [3] JOHANSSON L., EDLUND U., FAHLGREN A., ASPENBERG P., *Bone resorption induced by fluid flow*, Journal of Biomechanical Engineering, 2009, 131, CID 094505.
- [4] JOHANSSON L., EDLUND U., FAHLGREN A., ASPENBERG P., *Fluid induced osteolysis: modeling and experiments*, Computer Methods in Biomechanics and Biomedical Engineering, 2011, 14, 305–318.
- [5] EDWARDS J., *Physical characteristics of articular cartilage*, Proceedings of the Institution of Mechanical Engineers, 1966–1967, 181, 16–24.
- [6] GU W.Y., MAO X.G., FOSTER R.J., WEIDENBAUM M., MOW V.C., RAWLINS B.A., *The anisotropic hydraulic permeability of human lumbar annulus fibrosus – influence of age, degeneration, direction, and water content*, Spine, 1999, 24, 2449–2445.

- [7] MANSOUR J.M., MOW V.C., *The permeability of articular cartilage under compressive strain and high pressure*, The Journal of Bone and Joint Surgery (Am.), 1976, 58-A, 509–516.
- [8] McCUTCHEON C.W., *The frictional properties of animal joints*, Wear, 1962, 5, 1–17.
- [9] OSAMURA N., ZHAO C., ZOBITZ M.E., AN K., AMADIO P.C., *Permeability of the subsynovial connective tissue in the human carpal tunnel: a cadaver study*, Clinical Biomechanics, 2007, 22, 524–528.
- [10] PROCTOR C.S., SCHMIDT M.B., WHIPPLE R.R., KELLY M.A., MOW V.C., *Material properties of the normal medial bovine meniscus*, Journal of Orthopaedic Research, 1989, 7, 771–782.
- [11] WEISS J.A., MAAKESTAD B.J., *Permeability of human medial collateral ligament in compression transverse to the collagen fiber direction*, Journal of Biomechanics, 2006, 39, 276–283.
- [12] LEWIS J.L., KELLER C., STULBERG S.D., STEEGE J., SANTARE M., *The role of fluid hydrostatic pressure in bone–implant interface load transfer*, Annals of Biomedical Engineering, 1984, 12, 559–571.
- [13] FAHLGREN A., BOSTROM M.P.G., YANG X., JOHANSSON L., EDLUND U., AGHOLME F., ASPENBERG P., *Fluid pressure and flow as a cause of bone resorption*, Acta Orthopaedica, 2010, 81, 508–516.
- [14] HADDOCK S.M., DEBES J.C., NAUMAN E.A., FONG K.A., ARRAMON Y.P., KEAVENY T.M., *Structure–function relationships for coralline hydroxyapatite bone substitute*, Journal of Biomedical Research, 1999, 47, 71–78.
- [15] O'BRIEN F.J., HARLEY B.A., WALLER M.A., YANNAS I.V., GIBSON L.J., PRENDERGAST P.J., *The effect of pore size on permeability and cell attachment in collagen scaffolds for tissue engineering*, Technology and Health Care, 2007, 15, 3–17.
- [16] NETTI P.A., BERK A.B., SWARTZ M.A., GRODZINSKY A.J., RAKESH K.J., *Role of extracellular matrix assembly in interstitial transport in solid tumors*, Cancer Research, 2000, 60, 2497–2503.
- [17] ZNATI C.A., ROSENSTEIN M., MCKEE T.D., BROWN E., TURNER D., BLOOMER W.D., WATKINS S., JAIN K.J., BOUCHER Y., *Irradiation reduces interstitial fluid transport and increases the collagen content in tumors*, Clinical Cancer Research, 2003, 9, 5508–5513.
- [18] BOUCHER Y., BREKKEN C., NETTI P.A., JAIN R.K., *Intratumoral infusion of fluid: estimation of hydraulic conductivity and implications for the delivery of therapeutic agents*, British Journal of Cancer, 1998, 78, 1442–1448.
- [19] MILOSEVIC M., LUNT S.J., LEUNG E., SKLIARENKO J., SHAW P., FYLES A., HILL R.P., *Interstitial permeability and elasticity in human cervix cancer*, Microvascular Research, 2008, 75, 381–390.
- [20] MCGUIRE S., ZAHAROFF D., FANYUAN, *Nonlinear dependence of hydraulic conductivity on tissue deformation during intratumoral infusion*, Annals of Biomedical Engineering, 2006, 34, 1173–1181.